Pergamon

Geochimica et Cosmochimica Acta, Vol. 64, No. 5, pp. 835–847, 2000

0016-7037/00 $20.00 + .00

PII S0016-7037(99)00376-2

Fossil fish teeth as proxies for seawater Sr and Nd isotopes

E. E. MARTIN* and B. A. HALEY†

Department of Geological Sciences, 241 Williamson Hall, University of Florida, Gainesville, FL 32611-2120, USA

(*Received April* 20, 1999; *accepted in revised form September* 20, 1999)

Abstract—We analyzed Nd and Sr isotopic compositions of Neogene fossil fish teeth from two sites in the Pacific in order to determine the effect of cleaning protocols and burial diagenesis on the preservation of seawater isotopic values. Sr is incorporated into the teeth at the time of growth; thus Sr isotopes are potentially valuable for chemostratigraphy. Nd isotopes are potential conservative tracers of paleocirculation; however, Nd is incorporated post-mortem, and may record diagenetic pore waters rather than seawater. We evaluated samples from two sites (site 807A, Ontong Java Plateau and site 786A, Izu-Bonin Arc) that were exposed to similar bottom waters, but have distinct lithologies and pore water chemistries.

The Sr isotopic values of the fish teeth appear to accurately reflect contemporaneous seawater at both sites. The excellent correlation between the Nd isotopic values of teeth from the two sites suggests that the Nd is incorporated while the teeth are in chemical equilibrium with seawater, and that the signal is preserved over geologic timescales and subsequent burial. These data also corroborate paleoseawater Nd isotopic compositions derived from Pacific ferromanganese crusts that were recovered from similar water depths (Ling et al., 1997). This corroboration strongly suggests that both materials preserve seawater Nd isotope values. Variations in Pacific deepwater ε_{Nd} values are consistent with predictions for the shoaling of the Isthmus of Panama and the subsequent initiation of nonradiogenic North Atlantic Deep Water that entered the Pacific via the Antarctic Circumpolar Current. *Copyright © 2000 Elsevier Science Ltd*

1. INTRODUCTION

Ocean circulation directly impacts the redistribution of heat and nutrients on the earth. As a consequence, variations in ocean circulation in the past are tightly linked to global climate change. This is particularly apparent in the global response to openings and closings of major paleogeographic gateways. For example, Cenozoic development of the cryosphere has been linked to the opening of the Drake passage and the subsequent thermal isolation of Antarctica (Kennett, 1977; Kennett, 1982). In addition, closure of the Isthmus of Panama may have established conditions leading to the onset of Northern Hemisphere glaciation (Keigwin, 1982; Maier-Reimer et al., 1990; Hay, 1996; Haug and Tiedemann, 1998).

The precise correlation between paleocirculation and paleoclimate is difficult to document because there are few proxies that serve as true tracers of water mass. Current studies of paleocirculation are based on $\delta^{13}C$ (e.g., Shackleton et al., 1983; Curry et al., 1988; Woodruff and Savin, 1989; Raymo et al., 1990) and elemental ratios of Cd/Ca (Boyle and Keigwin, 1987; Boyle, 1988; Delaney, 1990); however, both of these proxies are influenced by nutrient cycling. As such, they reflect the age rather than the composition of a water mass. In addition, they can be affected by changes in productivity unrelated to circulation, such as global transfers between carbon reservoirs in the hydrosphere and geosphere. In contrast, Nd isotopes in seawater have been identified as conservative tracers of water mass (Piepgras and Wasserburg, 1982; Piepgras and Wasserburg, 1987; Piepgras and Jacobsen, 1988; Albaréde and Goldstein, 1992; Bertram and Elderfield, 1993; Jeandel, 1993; Shimizu et al., 1994; Jeandel et al., 1998).

One of the primary difficulties in exploiting Nd isotopes as a proxy for past water mass circulation is the identification of a common, dateable, marine phase that incorporates significant concentrations of deep water Nd and remains chemically inert during burial and lithification. A number of proxies have been tested with varying degrees of success, including biogenic calcite, inorganic phosphate, and several forms of ferromanganese deposits. All of these proxies, however, exhibit some limitations. In contrast, several studies suggest that fossil fish teeth do record bottom seawater Nd isotopes, as well as Sr isotopes (Staudigel et al., 1985; Grandjean et al., 1987; Snoeckx et al., 1995; Martin et al., 1995).

Some of the advantages of fish teeth are that they contain high concentrations of both Nd and Sr (100 to >1000 ppm Nd and >1000 ppm Sr; Wright et al., 1984; Shaw and Wasserburg, 1985; Staudigel et al., 1985; Martin et al., 1995), and they are found in sediment samples of all ages throughout the world's oceans. However, the hydroxyfluorapatite of fossil teeth contains 3 to 6 orders of magnitude more Nd than the hydroxyapatite of living fish teeth (Wright et al., 1984; Shaw and Wasserburg, 1985). This large increase requires post-depositional incorporation of Nd. An outstanding question, therefore, is whether the Nd isotopic compositions of the teeth are in equilibrium with seawater, pore water, or an intermediate mixture of the two fluids.

Previous studies have not rigorous tested the effect of pore water Nd on the preservation of the seawater signal in fossil fish teeth. The purpose of this paper is to further evaluate the influence of diagenesis and sample cleaning protocols on the extraction of deep seawater Nd and Sr isotopic values from fossil fish teeth. This has been accomplished by comparing Nd and Sr isotopes and concentrations in teeth for the past ~20 Ma

*Author to whom correspondence should be addressed (emartin@geology.ufl.edu).
†*Present address:* College of Oceanic and Atmospheric Sciences, Corvallis, OR 97331-5503, USA

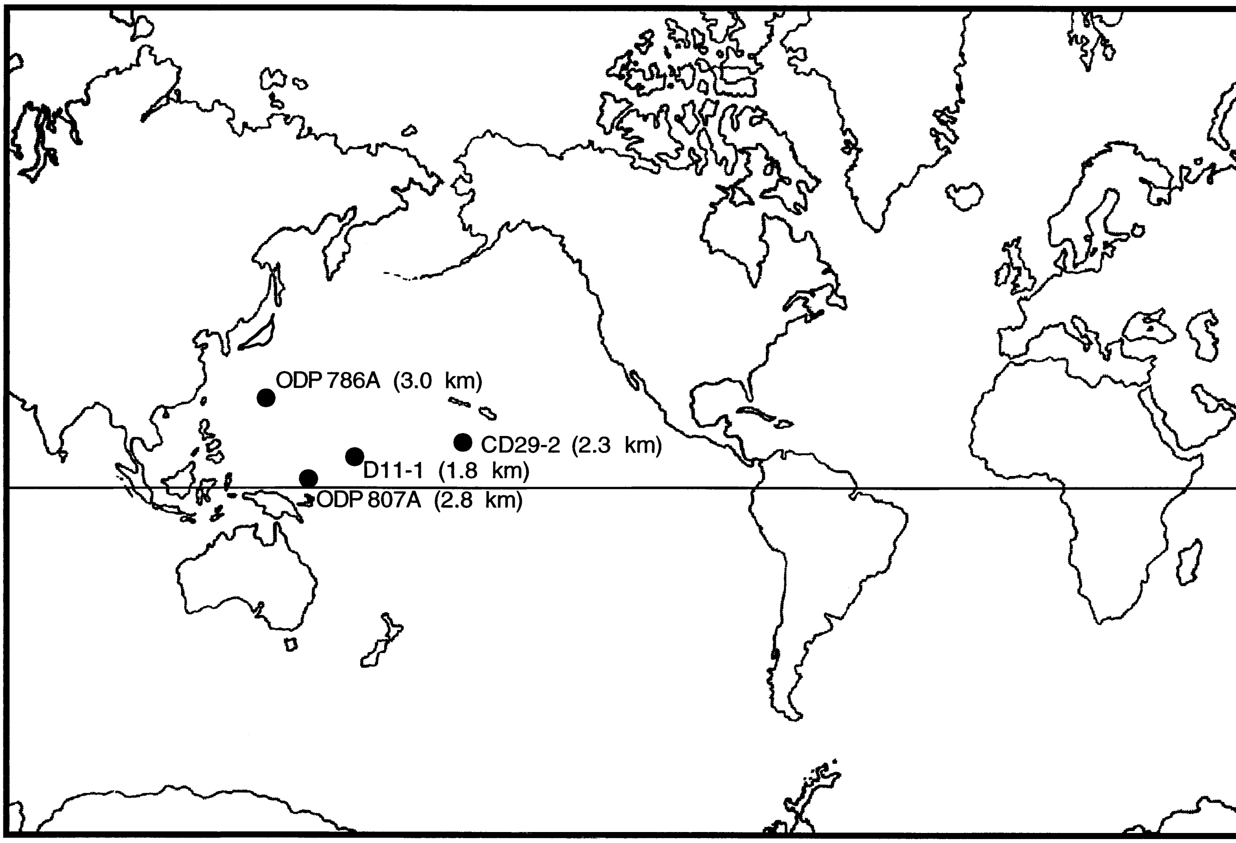

Fig. 1. Location map for sites discussed in the text. Numbers in parentheses represent modern water depths.

from two sites in the Western Pacific that have been exposed to similar bottom waters, but distinct pore waters. Data for reductively cleaned fossil fish teeth (Boyle, 1981; Boyle and Keigwin, 1985; Boyle, pers. commun., 1993) from sites 786A in the Izu-Bonin Arc and 807A on the Ontong-Java Plateau (Fig. 1) support the hypothesis that properly cleaned teeth yield seawater isotopic ratios, and that the teeth preserve that signal over geologic time scales and subsequent burial.

2. BACKGROUND

2.1. Seawater Nd

The seawater Nd budget is poorly constrained, but it is clear that the signal is dominated by continental inputs (Elderfield and Greaves, 1982; Goldstein et al., 1984; Goldstein and Jacobsen, 1988; Elderfield et al., 1990; Sholkovitz, 1993; Jeandel et al., 1995; Jones et al., 1994). Unlike the Sr system, the contribution from hydrothermal circulation along the mid ocean ridges appears to be negligible (Michard et al., 1983; Piepgras and Wasserburg, 1985; Goldstein and Jacobsen, 1988; Halliday et al., 1992; Bertram and Elderfield, 1993). The absolute value of the residence time of Nd in seawater can not be precisely defined (Elderfield and Greaves, 1982; Piepgras and Wasserburg, 1985; Jeandel et al., 1995), but the distinct isotopic values for different ocean basins and the systematic variations in isotopes with depth in the water column are evidence that the residence time must be shorter than the mixing time of the oceans (~1500 y; Broecker and Peng, 1982).

As a consequence of the short residence time and the dominance of continental sources, individual water masses can have distinct Nd isotopic signatures that reflect the geology of their source terranes plus variable degrees of mixing with other water masses. For example, NADW is characterized by relatively nonradiogenic ε_{Nd} values of ~ -14 (Piepgras and Wasserburg, 1987) (where ε_{Nd} represents deviations in parts per 10^4 of the $^{143}Nd/^{144}Nd$ ratio relative to the chondritic uniform reservoir (Jacobsen and Wasserburg, 1980)), reflecting the input of old cratonic material. In contrast, Pacific Deep Waters have ε_{Nd} values of ~ -4 (Piepgras and Jacobsen, 1988; Shimizu et al., 1994), reflecting the combination of Circum-Pacific arc volcanics and continental crust. Antarctic Circumpolar Water (ACW), which represents a mixture of these and other water masses, has an intermediate value of ~ -8 (Piepgras and Wasserburg, 1982; Jeandel, 1993).

2.2. Proxies for Bottom Water Nd Isotopes

A number of proxies have been evaluated in order to exploit the potential of Nd isotopes as tracers of paleocirculation, but all exhibit some limitation to their application. For biogenic calcite the primary problem is that Nd does not readily substitute in the calcite structure. Therefore, Nd concentrations are extremely low (<1ppm; Palmer, 1985), and Nd in the calcite tends to be overwhelmed by Nd in ferromanganese oxide coatings. In fact, Palmer and Elderfield (1985, 1986) used the ferromanganese coatings themselves to study secular variations in ε_{Nd} of seawater in the South Atlantic. Along these same lines, intriguing initial results have been reported from work on coatings from Recent and Pleistocene sediments (Rutberg et al., 1997; Hemming et al., 1998). In light of evidence that ferromanganese coatings continue to grow during burial diagenesis (Hein et al., 1997), more work is needed to demonstrate that these coatings preserve initial seawater values with time and burial.

Another form of ferromanganese oxide deposit that has been utilized is manganese nodules. It has been shown that Nd isotopes in Mn nodules recovered from surface sediments generally reflect the composition of the overlying water mass (Aplin et al., 1986/1987; Albaréde and Goldstein, 1992; Albaréde et al., 1997). Extremely slow growth rates (a few mm/m.y.; Ku and Broecker, 1967) suggest that the nodules yield an integrated signal of ocean chemistry over a long period of time (Elderfield et al., 1981).

Recently, a number of interesting studies have been published based on Nd isotopes preserved in hydrogenous ferromanganese crusts (Abouchami et al., 1997; Burton et al., 1997; Ling et al., 1997; O'Nions et al., 1998). These studies strongly support the conclusion that the major ocean basins have maintained their provinciality and stratification in terms of Nd isotopes for at least the past 20 Ma, and that there have been secular variations consistent with changes in ocean circulation. Although the results from these studies are very intriguing, particularly in the combination of Nd and Pb isotopes, they can not be considered conclusive because ferromanganese crusts also grow very slowly (<5 mm/m.y.). As a result, dating and high-resolution work are difficult. Dating for most studies is now based on $^{10}Be/^{9}Be$ techniques. This method is based on the assumption that the flux of ^{9}Be to the oceans has been constant through time and that diffusion of ^{10}Be is negligible. Furthermore, the short half-life of ^{10}Be limits the application of the technique to ~15 Ma. Ages for samples older than this must be extrapolated from more recent growth rates.

Another concern with the ferromanganese crust data is that the Sr isotopes are clearly altered (Ingram et al., 1990; VonderHaar et al., 1995; Ling et al., 1997; O'Nions et al., 1998). In addition, the distribution of ferromanganese crusts on the seafloor is spatially restricted. This becomes important because several studies suggest advective lengths of Nd may be shorter than expected (Abouchami et al., 1997; Ling et al., 1997; O'Nions et al., 1998). Samples located closer to important paleogeographic gateways may be necessary to monitor the maximum affect of these gateways on ocean circulation.

Another potential proxy for seawater Nd is inorganic phosphate (Shaw and Wasserburg, 1985; Stille and Fischer, 1990; Stille, 1992; Stille et al, 1996); however, the temporal distribution of this material is highly sporadic. They are abundant during some geologic time intervals, but rare during others, and they typically are limited to shallow marine environments. Therefore, they do not record the paleoceanographic history of deep marine circulation. Finally, there is evidence they may form interstitially (Burnett, 1990), implying they record pore water, rather than seawater values.

As mentioned, biogenic phosphates offer a number of advantages over the aforementioned proxies. They incorporate high concentrations of both Sr and Nd that appear to preserve seawater values, and they are widely distributed in time and space. Not all standard DSDP/ODP samples yield fish teeth; however, it is possible to increase the yield by concentrating on sites with low carbonate contents or sedimentation rates. Studies of biogenic phosphates can also be extended into the Paleozoic using conodonts, the phosphatic hardparts of a nektonic organism that became extinct in the Triassic (Wright et al., 1987; Keto and Jacobsen, 1987; Bertram et al., 1992; Martin and Macdougall, 1995; Felitsyn et al., 1998).

It is possible that the postdepositional increase in Nd (Wright et al., 1984; Shaw and Wasserburg, 1985; Staudigel et al., 1985; Martin et al., 1995) coincides with the rapid transition from the hydroxyapatite of living teeth to the hydroxyfluorapatite of fossil specimens found in surface sediments. Variations in Nd concentration with depth in the sediment support this idea of rapid incorporation. Fossil fish teeth recovered from the top few mm's of the sediment cores contain high concentrations of Nd, and there is no record of a systematic increase with burial (Bernat, 1975; Staudigel et al., 1985; Elderfield and Pagett, 1986; Wright et al., 1987). Additional data presented in this paper suggest the teeth record seawater isotopes even when sediment pore waters have a distinct chemistry, indicating that the incorporation occurs while the teeth are in contact with bottom water. An important advantage of this postmortem incorporation is that the life habitat of the fish (e.g., pelagic, benthic, migratory, etc.) becomes irrelevant. All teeth record Nd isotopes of bottom conditions, rather than water column values that vary with depth.

2.3. Site Descriptions and Pore Water Chemistries

Ocean Drilling Program (ODP) sites 807A on the Ontong Java Plateau (Leg130: 3°36.42′N, 156°37.49′E) and 786A at the Izu-Bonin Arc (Leg 125: 31°52.48′N, 141°13.58′E) (Fig. 1) are currently exposed to similar bottom waters. Assuming that general circulation patterns with respect to the two sites have not changed appreciably in the past 30 Ma, they should record a similar bottom water history. The Ontong Java Plateau is believed to have been bathymetrically stable for the past ~100 Ma (Resig et al., 1976). Its current water depth is 2803 m (Kroenke et al., 1991), which places it within upper Pacific Deep Water (PDW) (Pickard and Emery, 1990). Site 786A is currently at 3058 m (Fryer et al., 1990). Its calculated subsidence history places it at ~2000 m, roughly the boundary between PDW and Arctic Intermediate Water (AIW) (Pickard and Emery, 1990), at approximately 25 Ma (Bloomer et al., 1995). Therefore, it was also located in PDW throughout most of the time interval of interest for this study. The oldest samples, however, may have been influenced by AIW.

The primary differences between the two sites are the composition of the sediment and the associated differences in pore water chemistry. As is typical of all Ontong Java Plateau sediments, site 807A is composed of almost pure carbonate (92–93% $CaCO_3$). Drilling at this site penetrated to 1380 meters below seafloor (mbsf). All of the material sampled for this project comes from the upper 400 m of core, which places it all within lithologic Unit I, a Recent to the Eocene aged

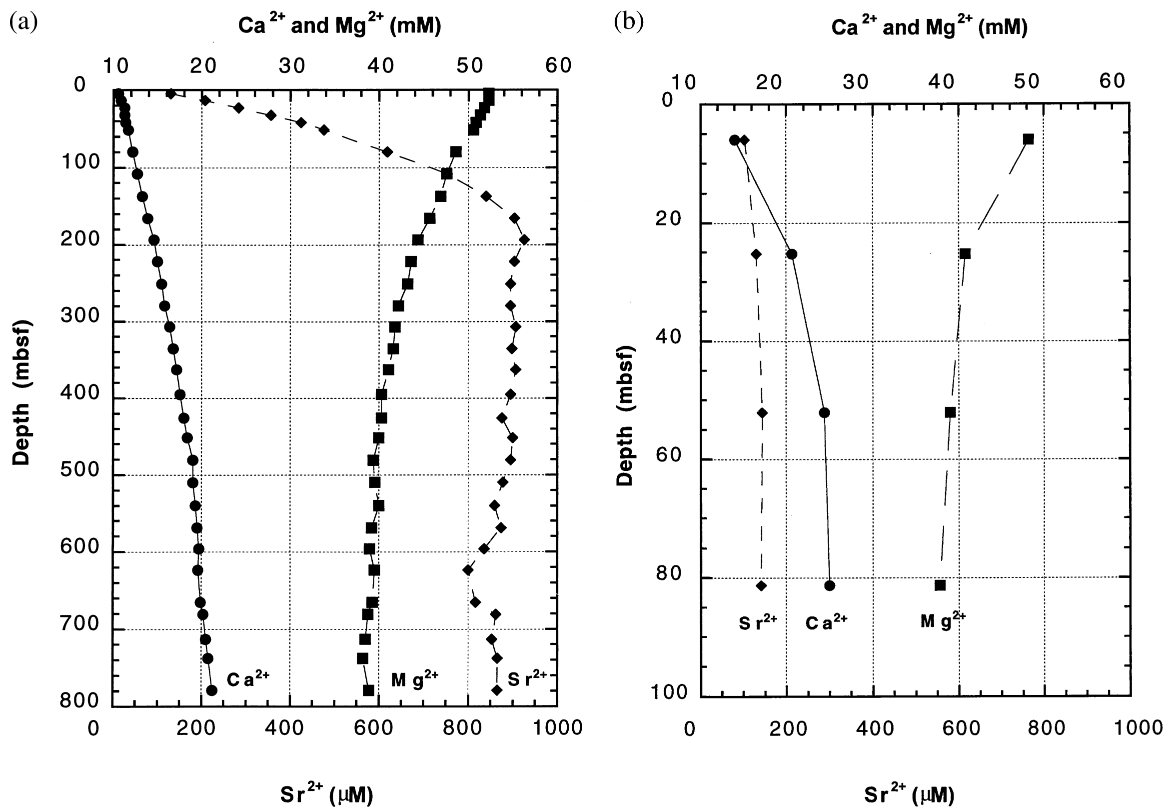

Fig. 2. Pore water profiles for Ca^{2+}, Mg^{2+} and Sr^{2+} for (a) site 807A, and (b) site 786A. Data for site 807A are from Kroenke et al. (1991). Data for site 786A are from Fryer et al (1990) and Mottl and Alt (1992).

foraminifera-rich, nannofossil ooze (Unit IA) and chalk (Unit IB). Wind-blown dust (Krissek and Janecek, 1993) and a minor amount of volcanic ash account for the noncarbonate fraction of the sediment. The ash occurs in thin layers defined by having >1% ash that are so discontinuous they cannot be correlated between neighboring sites (Kroenke, et al., 1991). Sedimentation rates for Unit I average 24.6 m/m.y. (Kroenke et al., 1991). Because of low remanent magnetic intensities, the age model for site 807A is based on nannofossil and foraminifera biostratigraphies (Berger et al., 1993).

Sediments from site 786A include a high proportion of volcanic ash because of the location near the Izu-Bonin arc. This site was drilled to a depth of 166 mbsf, but samples for this project only extend to 95 m. The sampled interval includes two lithologic units. Unit I extends from 0 to 83.4 mbsf (Pleistocene to middle Miocene) and includes all but the two deepest samples. This unit is described as nannofossil marls and clays with a persistent volcanogenic component (Fryer et al., 1990), which is found consistently throughout the unit as vitric particles and pumice fragments. In addition, there are 58 distinct ash layers. The base of Unit I is composed of a 10 cm thick layer of sideromelane and manganese oxide, which represents a hiatus of ~5 m.y. (Fryer et al., 1990). One of our samples (786; 9x-5) was collected from within this interval. Our two deepest samples come from Unit II (83.4–103.25 mbsf, late Oligocene to middle Eocene), which directly underlies the unconformity.

Sedimentation rates vary from ~4.4 to 7.2 m/m.y rates in Unit I to low values of 1 m/m.y. in Unit II. The units underlying Unit II are composed predominantly of volcanic breccias and flows. Because of poor recovery, drilling disturbances, and steeply dipping beds, paleomagnetic interpretations are limited to Pliocene and younger material. With the exception of these few points, the age model for site 786A is based on nannofossil biostratigraphy (Stabell et al., 1992). Errors associated with the age estimates are higher for Unit II due to the lower sedimentation rate.

The distinct lithologies at the two sites produce very different pore water chemistries. It is impossible to directly measure the effects of lithology on the Nd composition of the pore waters, because Nd concentrations in pore water is too low for analysis. However, other components, such as Ca^{2+} and Mg^{2+} concentrations and $^{87}Sr/^{86}Sr$ ratios, can be used to monitor diagenetic reactions between the solids and fluids. As Figure 2 illustrates, Ca^{2+} at site 807A increases while Mg^{2+} decreases with depth. The near linear Ca^{2+} and Mg^{2+} profiles for site 807A (Kroenke et al., 1991) indicate alteration of basaltic basement at depth, which serves as a source for Ca^{2+} and a sink for Mg^{2+}, with little evidence for reaction within the sediment column (McDuff and Gieskes, 1976). In contrast, a similar magnitude of change in Ca^{2+} and Mg^{2+}occurs over a much shorter depth interval at site 786A. The strong curvature of the site 786A profiles suggests reactions are occurring between the pore water and volcanic material within the sediment column. It is striking that this curvature is maintained given the slower sedimentation rates at site 786A.

Another measure of diagenetic alteration is pore water $^{87}Sr/$

Table 1. Sr isotope data for pore waters.

Sample	Age[a] (Ma)	$^{87}Sr/^{86}Sr_m$[b]	$^{87}Sr/^{86}Sr_{sw}$[c]	$\Delta^{87}Sr/^{86}Sr$[d]
807				
2–4	1.9	0.709042	0.709076	−0.000034
4–4	2.4	0.709012	0.709060	−0.000048
6–4	2.9	0.708952	0.709052	−0.000100
15–5	5.6	0.708935	0.708994	−0.000059
33–3	11.2	0.708785	0.708820	−0.000035
42–4	14.9	0.708633	0.708774	−0.000141
786				
3–4	3.6	0.708527	0.709046	−0.000520

[a] Ages are based on the timescale by Cande and Kent (1995).
[b] $^{87}Sr/^{86}Sr_m$ equals the measured $^{87}Sr/^{86}Sr$ of the pore water.
[c] Sr isotope values for contemporaneous seawater ($^{87}Sr/^{86}Sr_{sw}$) were derived from Farrell et al. (1995), Martin et al. (1999) and Hodell and Woodruff (1994).
[d] $\Delta^{87}Sr/^{86}Sr$ represents the Sr isotope value measured for the pore water minus the value measured for contemporaneous seawater.

^{86}Sr and Sr^{2+}values. The Sr^{2+} profile at site 807A (Fig. 2A) is typical of profiles controlled by recrystallization of biogenic calcite within the sediment column. There is a rapid increase to a maximum at depth followed by relatively constant values down to basement (e.g., Gieskes, 1981). At site 786A there is a slight increase in Sr^{2+} with depth, but the pore water data only extend to 81 mbsf. Pore water Sr isotope data are presented in Table 1. For site 807A the pore water $^{87}Sr/^{86}Sr$ values are 0.000034 to 0.000150 lower than those of contemporaneous seawater (Table 1). This presumably reflects upward diffusion of older Sr^{2+} from recrystallized calcite (Elderfield and Gieskes, 1982). The single pore water sample from site 786A shows a much greater $^{87}Sr/^{86}Sr$ deviation from contemporaneous seawater (0.000520; Table 1). This deviation is much greater than would be predicted based on modelling studies of carbonate recrystallization (Richter and DePaolo, 1988; Richter and Liang, 1993). Thus, the Sr isotopic data again suggest alteration of volcanic ash at site 786A. Volcanic breccias and flows at this site contain 100–200 ppm Sr with $^{87}Sr/^{86}Sr$ values of ~0.703 (Pearce et al., 1992).

In summary, the pore water chemistry at site 807A reflects carbonate diagenesis, while the chemistry at site 786A reflects alteration of volcanic ash. As mentioned, biogenic calcite has extremely low concentrations of Nd (Palmer, 1985; Palmer and Elderfield, 1986), therefore calcite diagenesis should not introduce significant Nd to the pore waters. In addition, any Nd introduced in this manner would have seawater-type Nd isotopes, implying that large amounts would be required to significantly alter the Nd isotope ratio of the pore water. In contrast, volcanic samples from site 786A contain 1–16 ppm Nd with ε_{Nd} values of +6 to +9 (Pearce et al., 1992), which are very distinct from seawater. Alteration of even a small amount of this material would increase the Nd isotopic ratio of the pore water.

The Ca^{2+} and Mg^{2+} profiles and pore water $^{87}Sr/^{86}Sr$ data do not provide definitive proof that ash alteration at site 786A is contributing radiogenic Nd to the pore waters, but they strongly suggest this is the case. If the Nd in fossil fish teeth is affected by pore water Nd, the preserved Nd isotope ratios for teeth from site 786A should be distinctly more radiogenic than those from site 807A. On the other hand, good agreement between site 786A and 807A fish teeth data would support the conclusion that the teeth preserve seawater isotopes.

3. METHODS

Fossil fish teeth were handpicked from the >125 μm fraction of sediment that was sonicated and sieved in distilled water. The weight and size of individual fish teeth were highly variable, with a single, complete tooth weighing from 10–215 μg. For site 786A we recovered enough teeth for analyses (~40 μg) from 8 of 18 samples. For site 807A there were enough teeth from 11 of 22 samples; 7 of the samples that did not yield teeth were from the chalk unit of 1B. The greater lithification of these samples made them more difficult to disaggregate and pick. The samples were initially distributed approximately every 1 m.y. from 0–15 Ma and every 5 m.y. from 15–40 Ma for both sites, but because many of the samples did not yield enough teeth, the final age distribution is less evenly distributed through time. Data from site 786A covers the range from 1.9–31 Ma based on the Cande and Kent (1995) timescale, and data from site 807A ranges from 1.7–14 Ma (Table 2 and Table 3).

One aspect of this study was to derive a cleaning procedure that would optimize the measurement of seawater Sr and Nd isotopes, and minimize contamination by sediment packed within the teeth, or oxide coatings on the surface of the teeth. These coatings may adhere to the teeth in the water column, on the sea floor, or after burial when they would be influenced by pore waters. Three separate cleaning procedures were applied to subsamples of the teeth:

1. sonication in quartz distilled water (labeled "u" for untreated);
2. leaching in 2 N acetic acid for approximately 20 min., or until they had lost ~15% by weight (labeled "l" for leached); and
3. reductive cleaning using a method designed to remove ferromanganese coatings (Boyle, 1981; Boyle and Keigwin, 1985) (labeled "c" for cleaned).

For the reductive cleaning, Boyle's original technique was modified by reversing the order of the oxidative and reductive steps (Boyle, pers. commun., 1993). Seven samples that were large enough to be subdivided were analyzed using 2 or 3 of these techniques.

Prepared teeth were dissolved in 1.8 N HCl, spiked for Sr and Sm/Nd concentration measurements, and dried. The samples were processed through cation-exchange column chemistry using standard techniques to separate Sr, Nd, and Sm. Blanks for this procedure were 91 pg for Sr, 6 pg for Nd and <1pg for Sm. Elemental concentrations were determined by isotope dilution thermal ionization mass spectrometry, and were measured simultaneously with $^{87}Sr/^{86}Sr$, and $^{143}Nd/^{144}Nd$. A number of samples did not run efficiently enough to collect sufficiently precise isotope ratios, but did yield accurate concentration data. These samples are listed in Table 2. Sm concentrations were measured for approximately half of the samples, including many of the oldest samples. $^{147}Sm/^{144}Nd$ values ranged from 0.11 to 0.15, and, as expected, the resulting corrections for post-mortem growth of radiogenic Nd were less than the stated uncertainty, thus no corrections were made for post-depositional growth of ^{143}Nd.

All of the Nd and eight of the Sr analyses were measured in dynamic mode on a Micromass Sector 54 at Scripps Institution of Oceanography. Nd samples of ~8 ng were loaded directly on a single Re filament in HCl and oxidized. The sample was then analyzed as NdO^+ at 0.35–0.4 V of ^{142}Nd for 300 ratios. All ratios are fractionation corrected to $^{148}Nd/^{144}Nd = 0.242436$. The $^{143}Nd/^{144}Nd$ value for repeat analyses of the La Jolla Nd standard by this method is 0.511859 ± 0.000014. In general, samples were only analyzed if the chemical separation of Sm, Nd, Pr, and Ce was such that interference corrections were not required for the $^{143}Nd/^{144}Nd$ ratio. However, four site 786A samples (786; 1-1c-i: 786; 1-3-u: 786; 5-3-u-i: 786; 5-3-l) did require small corrections for Pr interferences, but all corrections were less than the stated external precision of 0.000014. For all elements the spikes

Table 2. Nd concentration and isotope data.

Sample[a]	Sample interval	Depth (m)	Age[b] (Ma)	Wt (μg)	Nd (ppm)	$^{143}Nd/^{144}Nd$[c]	ε_{Nd}[d]	ε_{Nd} error
786A								
1-1-*c-i*	1H-1, 147–150	1.5	1.9	49	728	0.512488 ± 9	−2.93	0.18
1-3-*c-i*	1H-3, 18–22	3.2	2.3	60	400	0.512548 ± 13	−1.76	0.25
1-3-*c-ii*	1H-3, 18–22	3.2	2.3	87	437	0.512510 ± 10	−2.50	0.20
1-3-*u*	1H-3, 18–21	3.2	2.3	52	555	0.512504 ± 10	−2.61	0.20
3-CC-*c*	3H-cc, 17–21	28.7	4.8	25	668	0.512446 ± 9	−3.75	0.18
5-3-*c-i*	5x-3, 13–17	41.3	7.4	53	554	0.512486 ± 11	−2.97	0.21
5-3-*c-ii*	5x-3, 10–14	41.3	7.4	80	521	0.512497 ± 13	−2.75	0.25
5-3-*u-l*	5x-3, 13–17	41.3	7.4	64	385	0.512534 ± 10	−2.03	0.20
5-3-*u-ii*	5x-3, 10–14	41.3	7.4	88	416	—		
5-3-*l*	5x-3, 13–17	41.3	7.4	53	444	0.512500 ± 8	−2.69	0.16
5-4-*c*	5x-4,	43.5	8.5	93	895	0.512488 ± 9	−2.93	0.18
8-1-*c*	8x-1, 28–38	67.4	14.3	79	196	0.512450 ± 18	−3.67	0.35
8-1-*c*	8x-1, 28–38	67.4	14.3	79	196	0.512460 ± 12	−3.47	0.23
8-1-*u*	8x-1, 28–38	67.4	14.3	45	286	0.512485 ± 10	−2.98	0.20
8-1-*l*	8x-1, 28–38	67.4	14.3	40	359	0.512492 ± 9	−2.85	0.18
9-5-*c-i*	9x-5, 59–65	83.4	16.8–23.8	46	430	0.512608 ± 9	−0.59	0.18
9-5-*c-ii*	9x-5, 58–66	83.4	16.8–23.8	158	755	—		
9-5-*c-iii*	9x-5, 58–66	83.4	16.8–23.8	114	1168	0.512396 ± 8	−4.72	0.16
9-5-*c-iv*	9x-5, 58–66	83.4	16.8–23.8	113	581	0.512419 ± 10	−4.27	0.20
9-5-*u-i*	9x-5, 58–66	83.4	16.8–23.8	139	1081	0.512422 ± 9	−4.21	0.18
9-5-*u-ii*	9x-5, 58–66	83.4	16.8–23.8	91	885	—		
9-CC-*c*	9x-cc, 7–11	85.1	24.9	83	270	0.512474 ± 10	−3.20	0.20
10-4-*c-i*	10x-4, 140–144	92.3	31.2	27	196	0.512637 ± 9	−0.02	0.18
10-4-*c-ii*	10x-4, 137–140	92.3	31.2	77	452	0.512607 ± 9	−0.60	0.18
807A								
3-CC-*c*	3H-cc, 3–10	26.2	1.7	49	141	0.512497 ± 11	−2.75	0.21
5-CC-*c*	5H-cc, 0–10	45.3	2.6	210	116	0.512471 ± 9	−3.26	0.18
5-CC-*c*	5H-cc, 0–10	45.3	2.6	210	116	0.512478 ± 12	−3.12	0.23
5-CC-*u*	5H-cc, 0–10	45.3	2.6	37	346	0.512479 ± 11	−3.10	0.21
5-CC-*l*	5H-cc, 0–10	45.3	2.6	46	699	0.512452 ± 10	−3.63	0.18
7-CC-*c*	7H-cc, 3–9	64.3	3.3	75	302	0.512510 ± 10	−2.50	0.20
12-CC-*c*	12H-cc, 7–9	111.5	4.9	26	330	—		
14-CC-*c-i*	14H-cc, 0–6	130.7	5.5	68	339	—		
14-CC-*c-ii*	14H-cc, 0–9	130.7	5.5	32	256	—		
14-CC-*u*	14H-cc, 0–6	130.7	5.5	53	215	—		
16-CC-*c-i*	16H-cc, 4–10	149.8	6.1	36	323	—		
16-CC-*c-ii*	16Hcc, 11–13	149.9	6.1	39	278	0.512476 ± 12	−3.16	0.23
25-CC-*c-i*	25H-cc, 0–6	235.3	8.3	28	334	—		
25-CC-*c-ii*	25H-cc, 7–10	235.3	8.3	53		—		
25-CC-*u*	25H-cc, 7–10	235.3	8.3	63	310	0.512470 ± 10	−3.28	0.20
29-CC-*c-i*	29x-cc, 0–6	273.5	9.4	35	165	—		
29-CC-*c-ii*	29x-cc, 23–25	273.8	9.4	39	234	0.512476 ± 10	−3.16	0.20
32-CC-*c*	32x-cc, 6–12	300.5	10.9	59	304	—		
37-CC-*c*	37x-cc, 0–12	349.9	13.1	70	156	0.512459 ± 10	−3.49	0.20
41-CC-*c*	41x-cc, 0–6	389.0	14.0	36	189	—		

[a] Letters in italics indicate the cleaning technique used. See text for complete description. c = cleaned, u = untreated, l = leached.
[b] Ages are based on the timescale by Cande and Kent (1995).
[c] The $^{143}Nd/^{144}Nd$ value for the La Jolla standard is 0.511859. The ± uncertainty × 10^6 represents the within-run uncertainty. For the purposes of comparison all samples have been assigned a minimum uncertainty of 0.000014.
[d] $\varepsilon_{Nd} = [^{143}Nd/^{144}Nd_{(sa)}/^{143}Nd/^{144}Nd_{(CHUR)} - 1] \times 10^4$, where $^{143}Nd/^{144}Nd_{(CHUR)} = 0.512638$.

were pure enough that errors in weighing did not alter the spike corrected isotope ratio.

For Sr analyses, ~25 ng of Sr was loaded in tantalum oxide on a single tungsten filament and analyzed at 1.5 V of ^{88}Sr for 300 ratios. The long term mean and total variability of NBS 987 for Scripps is 0.710260 ± 0.000023. These stated external precisions represent the minimum uncertainty assigned to any sample. Within-run uncertainties were generally smaller, and have been listed in Tables 2 and 3. Thirteen additional Sr samples were analyzed in dynamic mode on a Finnegan 262 at Florida State University (FSU). These samples were loaded on tungsten filaments using a technique modified from Birck (1986) and analyzed at 1.2 V of ^{88}Sr for 150 ratios. All ratios were fractionation corrected to $^{86}Sr/^{88}Sr = 0.1194$. The interlaboratory calibration for these samples is complicated by the fact that FSU normally runs E&A for its laboratory standard. The long-term mean and 2σ uncertainty for this standard is 0.708000 ± 0.000020. For the purpose of calibration, two NBS 987 standards were run with the samples at FSU and three samples (786; 5-3-c-i: 786; 9-5-u-i: 807; 37-CC-c) were run in both laboratories (Table 3). The average difference between NBS 987 values and between the replicates was used to correct the samples for interlaboratory bias, then all of the samples were corrected to the University of Florida NBS 987 value of 0.712035 ± 0.000023 for correlation with seawater data from UF. This standard value represents 110 analyses of NBS 987 over a period of several years, and the external precision is equivalent to the total variability of analyses.

Table 3. Sr concentration and isotope data.

Sample[a]	Age[b] (Ma)	Wt (mg)	Sr (ppm)	$^{87}Sr/^{86}Sr$[c]	Error[d]
786A					
1-1-*c-i*	1.9	49	1821	0.709069	0.000045
1-3-*u*	2.3	52	1890	*0.709035*	0.000017
5-3-*c-i*	7.4	53	1637	*0.708868*	0.000019
5-3-*c-ii*	7.4	80	1623	0.708853	0.000013
5-3-*u-ii*	7.4	88	1803	0.708857	0.000010
5-4-*c*	8.5	93	1981	*0.708855*	0.000016
9-5-*c-iii*	16.8–23.8	114	2023	*0.708262*	0.000020
9-5-*u-i*	16.8–23.8	139	2211	0.708254	0.000035
9-5-*u-i*	16.8–23.8	139	2200	*0.708234*	0.000020
9-5-*u-ii*	16.8–23.8	91	2243	*0.708296*	0.000017
9-CC-*c*	24.9	83	1785	*0.708265*	0.000014
10-4-*c-ii*	31.2	77	1943	*0.708076*	0.000018
807A					
7-CC-*c*	3.3	75	3055	*0.709145*	0.000016
16-CC-*c-ii*	6.1	39	5418	*0.708930*	0.000017
25-CC-*c-i*	8.3	28			
25-CC-*c-ii*	8.3	53	4652	0.708874	0.000007
25-CC-*u*	8.3	63	5118	0.708880	0.000011
29-CC-*c-ii*	9.4	39	5119	0.708851	0.000011
32-CC-*c*	10.9	59	4108	*0.708857*	0.000025
37-CC-*c*	13.1	70	4513	0.708795	0.000024
37-CC-*c*	13.1	70	4617	*0.708792*	0.000030

[a] Letters in italics indicate cleaning protocol applied to the sample. See Table 2 and text for more details.

[b] Ages are based on the timescale by Cande and Kent (1995).

[c] Isotopic ratios listed in italics were analyzed at Florida State University. All other samples were analyzed at Scripps Institution of Oceanography. All data have been normalized to an NBS 987 value of $^{87}Sr/^{86}Sr = 0.710235$.

[d] The errors listed represent the within-run uncertainty. For plotting all samples were assigned a minimum external precision of 0.000023.

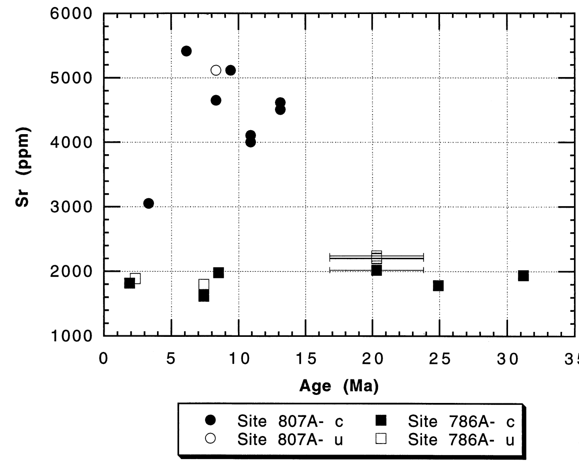

Fig. 3. Sr concentration data for ‘untreated’ (u) and ‘cleaned’ (c) fossil fish teeth from sites 807A and 786A. Each site has a distinct and limited range of concentrations.

4. RESULTS AND DISCUSSION

4.1. Cleaning Techniques

One of the primary goals of this study was to determine the cleaning protocol required to produce the most accurate seawater Sr and Nd data. Results for Sr from three sets of samples with reductively cleaned and untreated subsamples suggest that cleaning has little effect on the Sr system (Fig. 3, Table 3). There was a small decrease in Sr concentration of 8 to 25% associated with the cleaning. For comparison, concentrations for replicate samples prepared using the same technique always agreed within 5%. The $^{87}Sr/^{86}Sr$ value of all subsamples agreed within error regardless of the cleaning technique (Fig. 4), indicating that cleaning had no effect on the Sr isotopic composition.

The cleaning method, however, appears to affect Nd concentrations and isotopic ratios. Seven samples were subdivided to compare results of reductively cleaned and untreated samples. Three of these samples were further subdivided to test the effect of leaching. The acetic leached samples tended to have the highest Nd concentrations followed by the untreated subsamples (Fig. 5, Table 2). This suggests that the ferromanganese oxides removed by the reductive cleaning have higher concentrations of Nd than the fish teeth. Because these oxides are not as soluble in acetic acid, leaching may preferentially remove the fish tooth apatite, thereby effectively concentrating the Nd from the ferromanganese oxide.

The ε_{Nd} values of half of the reductively cleaned subsamples at site 786A are less radiogenic by more than uncertainty compared to values for untreated subsamples (Fig. 6, Table 3). The other half of the site 786A pairs and the single site 807A pair have ε_{Nd} values that agree within error. Also, one unpaired, untreated sample from site 807A (25-CC-u, 8.3 Ma) agrees well with reductively samples of a similar age. This pattern supports the idea that the material removed from site 786A samples during cleaning may have been influenced by radiogenic Nd from pore waters, while material removed from site 807A samples did not appear to have been altered. Based on these results we conclude that the best approach is to put all samples through Boyle’s reductive cleaning technique (Boyle, 1981; Boyle and Keigwin, 1985; Boyle, pers. commun., 1993). We would also recommend that future studies focus on sites that do not have high concentrations of sedimentary components that could contribute Nd to the pore fluid system.

4.2. Sr Concentrations

Sr concentration data (Fig. 3) illustrate that each site defines a distinct population. Concentrations for site 786A samples range from 1600 to 2250 ppm, while all samples at site 807A have concentrations greater than 3000 ppm; in fact, all but one (807; 7-CC-c; 3.3 Ma) have concentrations greater than 4000 ppm. There is a trend toward decreasing concentration with age (depth) in the site 786A samples, but no similar trend in the site 807A data.

One possible explanation for the bimodal Sr concentration data is that the teeth from site 807A have been diagenetically altered in the Sr-rich pore fluids observed at that site. The rapid sedimentation rates at site 807A resulted in deep burial depths, which could lead to a greater diagenetic potential. However, several lines of evidence suggest diagenesis is not the cause of the high concentrations. In particular, Shemesh (1990) found that Sr concentrations decreased as the hydroxyapatite of the teeth recrystallized to more stable mineralogies, which may

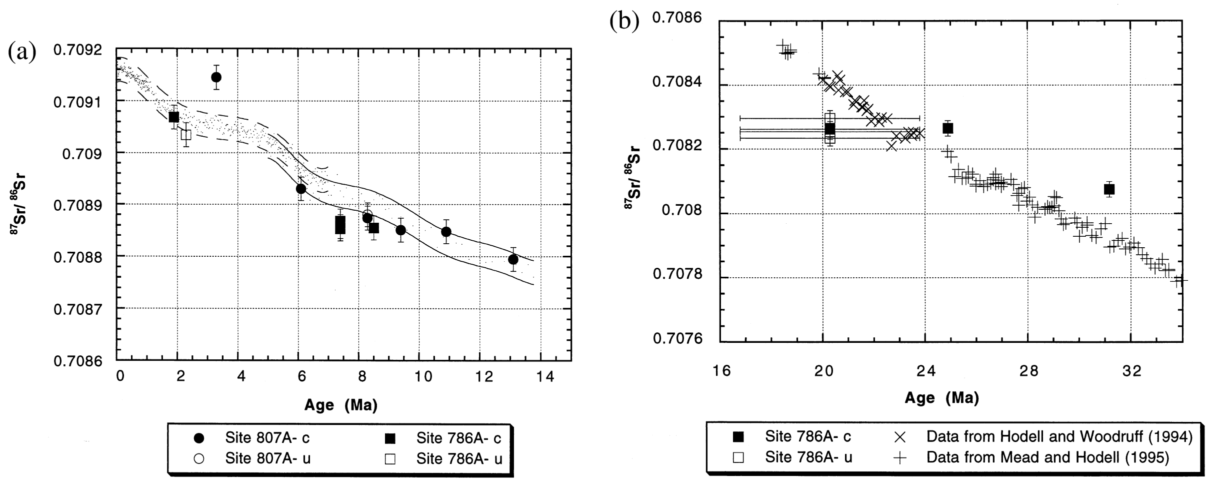

Fig. 4. Sr isotope data for 'untreated' (u) and 'cleaned' (c) fossil fish teeth from sites 807A and 786A compared to the seawater curve for (a) 0–14 Ma, and (b) 16–32 Ma. The dashed lines outline the error envelope for the curve by Farrell et al. (1995), the solid lines outline the error envelope for the curve by Martin et al. (1999).

account for the decreasing trend observed with depth at site 807A. But it is difficult to reconcile diagenesis as the cause of both very high concentrations and decreasing concentrations with depth. In addition, Richter and DePaolo (1988) demonstrated that, in the case of carbonate sediments, the rate of diagenesis is controlled by age rather than depth. Although this may not apply to phosphatic material, it suggests that more rapid burial rates would not result in greater diagenesis.

Another possible explanation of the bimodal Sr concentration data is that different populations of fish inhabited the two sites. Sites 807A and 786A are separated by ~30 degrees of latitude. Differences in the water temperatures at the two sites would create conditions favorable to different genera of fish, which might incorporate different concentrations of Sr into their teeth. The range of concentrations observed at site 786A are consistent with limited published data on Sr concentrations in modern and fossil teeth, as well as data collected from modern teeth during this study. Schmitz et al. (1991) reported a value of 1630 ppm Sr for a modern shark's tooth. Teeth from a trigger fish and a thresher shark analyzed during this study contained 950 and 1600 ppm Sr respectively. These data also agree with values observed in Cenozoic fossil teeth recovered from deep sea sediments (Staudigel et al., 1985). Yet none of these values are as high as those observed at site 807A, which averaged 4550 ppm. The only reported values that approach the site 807A concentrations are from studies of Cenozoic and Mesozoic teeth from sections currently exposed on land (Grandjean et al., 1987; Schmitz et al., 1991). These studies report concentrations up to 5580 ppm Sr, but average 2000–3000 ppm. The correlation between higher concentrations and older, Mesozoic and Cenozoic, teeth might again suggest alteration as the cause of high concentrations, if there were a mechanism to both increase and decrease Sr concentrations during recrystallization. Because we can not identify any such

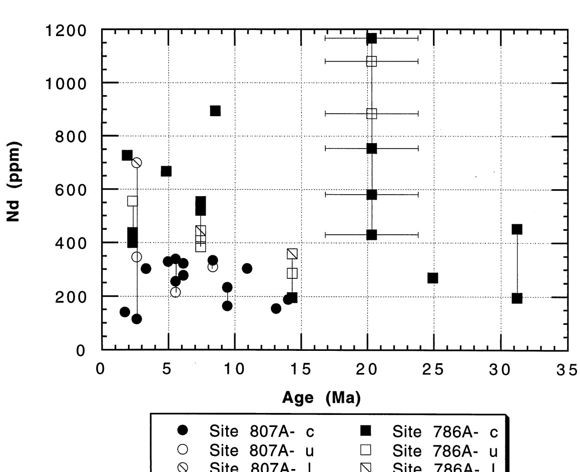

Fig. 5. Nd concentration vs. age for 'untreated' (u), 'cleaned' (c) and 'leached' (l) fish teeth samples from sites 786A and 807A. Vertical lines connect subsamples.

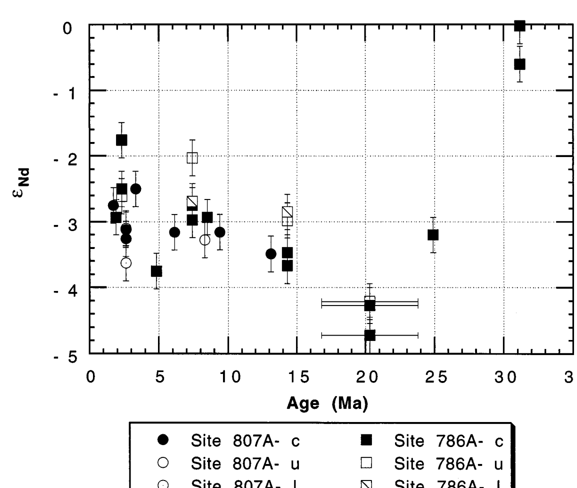

Fig. 6. ε_{Nd} vs. age for 'untreated' (u), 'cleaned' (c) and 'leached' (l) fish teeth samples from sites 786A and 807A.

mechanism, we believe the Sr concentrations observed in the teeth from sites 807A and 786A reflect the original concentrations incorporated into the teeth, and that the concentrations at site 807A represent the extreme end-member of a limited data set.

4.3. Sr Isotopes and Chemostratigraphy

Sr isotope ratios of the fossil fish teeth are compared to published seawater data in Figure 4. The solid and dashed lines on Figure 4a outline the window of uncertainty from published seawater curves (Farrell et al., 1995; Martin et al., 1999). The fish teeth data generally plot within error of the published data. Only one sample from site 807A plots outside of this error (807; 7CC-c; 3.3 Ma), and this sample has an anomalously low Sr concentration as well. Unfortunately, a replicate analysis of this sample was not possible because of the limited sample size. Samples from Unit I at site 786A (Fig. 4a) either plot within error of the seawater curve or are slightly less radiogenic. In contrast, samples from Unit II at this same site tend to be considerably more radiogenic than seawater values (Fig. 4b). This is surprising in view of the fact that analyses of volcanic material and pore waters (Table 1) from site 786A yield $^{87}Sr/^{86}Sr$ values that are much less radiogenic than contemporaneous seawater (Pearce et al., 1992). Thus, diagenetic alteration of the fish teeth in this environment should result in less radiogenic Sr isotopic values.

The offset between the Sr isotopic data for the fish teeth and the seawater curve may be due to the biostratigraphic age model and the slow sediment rate for Unit II. The reported age of 31.1 Ma for sample 786; 10-4 was derived by fitting a linear regression to the nannofossil datums below the hiatus represented by the sideromelane/manganese oxide layer (Stabell et al., 1992), and then converting the ages to the timescale by Cande and Kent (1995) using Mead (1996). Examination of the nannofossil data for site 786A (Xu and Wise, 1992) illustrates that from section 10x-1 to 10x-6, only one nannofossil sample was evaluated for each section of core. In other words, there is only one sample per 1.5 m, or one sample every 1.5 m.y. at the given sedimentation rate. A reasonable estimate of the potential error in age, therefore, is ± 1.5 Ma, indicating that the sample could be as young as 29.6 Ma, which would place it just above the seawater curve (Fig. 4b). In addition, the initial biostratigraphic age model for the site (Fryer et al., 1990) yielded an age of 28.65 Ma for this sample, which places it on the curve. A similar situation occurs for sample 786; 9cc. In this case, the plotted age of 24.9 Ma was derived from the Stabell et al. (1992), but data from the Initial Site Report (Fryer et al., 1990) placed it at 23.7 Ma, which again would move it onto the seawater curve.

Assuming that the radiogenic Sr values in Unit II of site 786A are a function of uncertainties in the age model, which are compounded by the low sedimentation rate, the general correlation between $^{87}Sr/^{86}Sr$ data for the fish teeth and published seawater curves suggests that fossil fish teeth are relatively reliable recorders of seawater Sr isotopes (Fig. 4). If the fish teeth do record seawater values at the time of formation, Sr isotope stratigraphy offers a means of determining the age of the teeth within the sideromelane/manganese oxide layer that represents the hiatus. Although this layer is placed in the middle Miocene unit (Fryer et al., 1990), the Sr data indicate a late Oligocene age (Fig. 4b).

4.4. Nd Concentrations

The two sites also define two populations based on their Nd concentrations (Fig. 4). Concentrations of reductively cleaned and untreated samples from site 807A range from ~100 to 350 ppm, while samples from site 786A range from ~200 to 1150 ppm. It is important to note that concentrations do not increase with burial depth or age. In fact, there is a slight trend toward decreasing values at both sites.

Unlike the bimodal Sr concentration data, which was attributed to pre-depositional processes, the distinct Nd concentrations observed at the two sites (Fig. 5) must be related to post-depositional incorporation, or conditions on the seafloor. Assuming seawater is the primary source of Nd incorporated into the teeth, variations in concentration could be related to sedimentation rate as proposed by Elderfield et al. (1981) for ferromanganese nodules and Elderfield and Pagett (1986) for fish teeth. Site 786A does have the highest concentrations and the lowest sedimentation rates. However, this correlation breaks down within site 786A. Sedimentation rates were much lower prior to the hiatus in site 786A, but Nd concentrations are similar throughout the core, and are even slightly lower in the sediments from Unit II that were deposited at the slowest rates.

Sample 786; 9-5 (16.8–23.8 Ma) exhibits a wide range of Nd concentrations. This sample comes from the sideromelane/manganese oxide layer that represents the ~5 m.y. hiatus. Biota from the upper portion of the sample interval indicate ages of 16.8 Ma, while biota from the lower portion of the same sample suggest an age of 23.8 Ma (Stabell et al., 1992), which is consistent with the Sr isotope chemostratigraphy. Presumably, fish teeth collected from this integrated sample may represent any age within that range, and also may have been exposed to seawater for varying lengths of time.

Bernat (1975), Staudigel et al. (1985), Elderfield and Pagett (1986) and Grandjean et al. (1987) all demonstrated that Nd concentrations in fish teeth do not increase with burial depth and age, indicating that Nd is incorporated into the teeth during very early diagenesis while the teeth are still in contact with seawater, and that there is little additional incorporation during burial. The lack of increasing concentrations with depth observed in our data supports this conclusion. As Staudigel et al. (1985) pointed out, the teeth can attain very high concentrations of Nd, up to at least 3800 ppm. Thus, they are not likely to be saturated with respect to Nd at the concentration levels reported in this study. The fact that there does not appear to be continuous incorporation of Nd during early diagenesis and burial is probably due to the limited availability of REE in the pore waters (Staudigel et al., 1985). It should be noted that Site 786A, which has the highest concentrations, is also the site with abundant volcanic ash, a potential source of Nd to the pore waters. Therefore the concentration differences between the two sites would be consistent with potential effects of diagenesis. However, the Nd isotope data, presented below, do not support this conclusion. The isotopes record a remarkable correlation between the two sites, as well as published data. In addition, there is no correlation between concentration and Nd isotopes. These observations suggest that any diagenetic effects are minor.

4.5. Nd Isotopes and the Record of Paleocirculation

ε_{Nd} values from the two sites range from -5 to -1.75, with the exception of the oldest sample from Site 786A (Fig. 6). There is an excellent correlation between reductively cleaned samples from site 786A and both cleaned and untreated samples from site 807A. In general, these samples indicate that Nd isotopes of deep to intermediate Central Pacific waters increased from ~-4.0 ε_{Nd} units at 20 Ma to -2.5 ε_{Nd} units at $\sim$4 Ma. Samples younger than 2.3 Ma indicate a decreasing trend toward modern values of -3.5 (Piepgras and Jacobsen, 1988; Ling et al., 1997; Shimizu et al., 1994).

There are a few samples that do not fit this general trend. Sample 786; 1-3-c-i (2.3 Ma) is significantly more radiogenic ($\varepsilon_{Nd} = -1.8$) than replicate reductively cleaned or untreated subsamples, as well as all other data of a similar age. Sample 786; 3-CC-c (4.8 Ma) is very unradiogenic relative to samples of similar age, but because of sample limitations we were unable to replicate this sample. Although both data points are suspect, neither is so far from the general curve that they alter the basic trends.

Sample 786; 9-CC-c (24.9 Ma) is quite radiogenic compared to site 786; 9-5 (16.8–23.8 Ma) samples. Interestingly, the subsidence history places site 786A near the modern depths for the boundary between PDW and AIW at $\sim$25 Ma. ε_{Nd} values for AIW are approximately 2 ε_{Nd} units higher than PDW (Piepgras and Jacobsen, 1988; Shimizu et al., 1994), therefore, the more radiogenic values of this sample may represent mixing between these two water masses.

Nd isotopes for sample 786; 10-4 (31.2 Ma) are significantly more radiogenic than any modern water mass with the exception of Pacific surface water ($\varepsilon_{Nd} = \sim0$; Piepgras and Jacobsen, 1988; Shimizu et al., 1994). Replicates for this interval were taken from sediment samples separated by a few cm's, cleaned in separate batches, and analyzed at different times. These reproducible, radiogenic values imply that the teeth are recording a unique water composition. One possible source of this unique fluid is the underlying volcaniclastics and flows (>800 m thick) that grade downward into basaltic basement. The fish teeth ε_{Nd} values may have been influenced by fluids expelled from this volcanic material into local bottom water at the time of deposition, or they may have been diagenetically altered by deeper pore waters during burial and diagenesis of the volcanic material. This is a subtle distinction, but it has

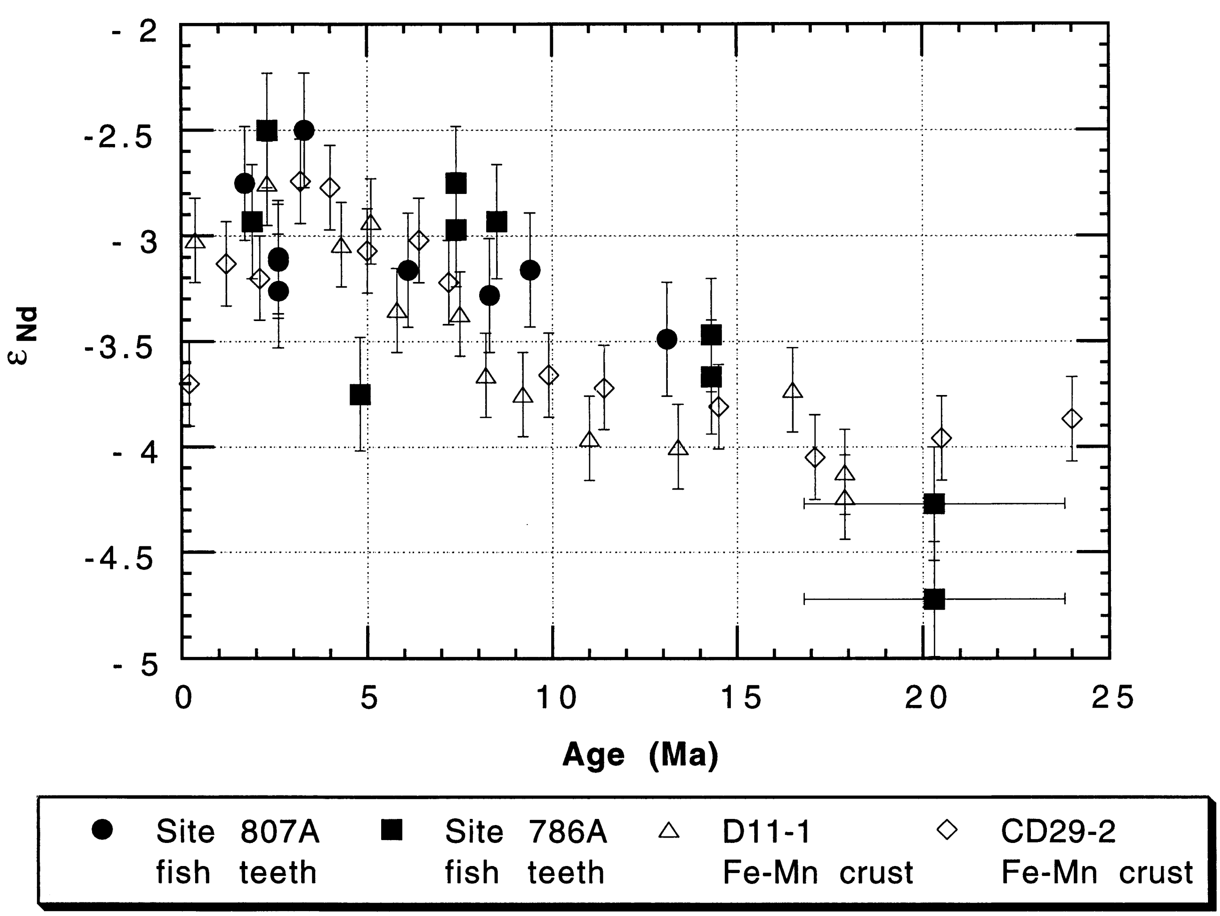

Fig. 7. A comparison of ε_{Nd} vs. age for 'untreated' (u) and 'cleaned' (c) fish teeth from site 807A, 'cleaned' fish teeth from site 786A, and ferromanganese crusts from Ling et al. (1997) for the past 25 Ma.

significant implications for the timing of Nd incorporation into fish teeth, and the likelihood that the teeth record paleoseawater chemistry.

As discussed earlier, depending on the age model applied, Sr isotopes for sample 786; 10-4 (31.2 Ma) may be more radiogenic than, or roughly equivalent to, contemporaneous seawater. In contrast, basaltic pore fluids should shift the Sr isotopes toward less radiogenic values. This decoupling of the Sr and Nd systems suggests that the offset in the Sr and Nd signatures is not purely diagenetic porewaters. It implies that the teeth are recording the original seawater Sr incorporated during the life of the fish, while the Nd represents bottom waters at the time of deposition, albeit bottom waters that have been influenced by basaltic fluids. Because it is clear that the Nd data from 786; 9CC-c (24.9 Ma) and 786; 10-4 (31.2 Ma) do not represent deep water, they are excluded from further discussion.

Figure 7 illustrates the excellent correlation between the Nd isotope data from sites 786A and 807A and the data from ferromanganese crusts published by Ling et al. (1997). The fact that two different proxies of seawater Nd isotopes produce such similar records argues for the integrity of both proxies.

Although there is excellent agreement between all of the sites shown in Fig. 7, there is a tendency for the fish teeth data to plot slightly higher, but within error, of the crust data. This trend is the opposite of what would be expected based on water depths. The fish teeth sites are from slightly greater modern water depths, implying that if they are different, they should have slightly more negative values (Piepgras and Wasserburg, 1987; Piepgras and Jacobsen, 1988; Bertram et al., 1993; Jeandel, 1993; Jones et al., 1994). This offset is in the right direction to represent an influence from altered pore waters at site 786A; however, site 807A shows a similar offset. Alternatively the offset may be due to an interlaboratory bias.

As suggested by Burton et al. (1997), Ling et al. (1997) and O'Nions et al. (1998), the progressively more radiogenic ε_{Nd} values from 15 to 4 Ma probably reflect decreasing flow of nonradiogenic Atlantic waters into the Pacific as the Isthmus of Panama shoaled, as modeled by Maier-Reimer et al. (1990), Mikolajewicz et al. (1993) and Mikolajewicz and Crowley (1997). The subsequent decreasing values probably record the intensification of nonradiogenic NADW production. This water then entered the Pacific via the ACC (Abouchami et al., 1997), producing more nonradiogenic Nd values from 4 Ma to present.

5. CONCLUSIONS

Nd isotopes preserved in cleaned fossil fish teeth appear to be accurate recorders of bottom seawater Nd isotopes. This is true even in the case of site 786A where pore waters presumably include Nd that is isotopically distinct from seawater. Nd isotopes preserved in fossil fish teeth from the Pacific also agree well with values preserved in ferromanganese crusts; suggesting both phases are accurate proxies for seawater Nd. Unlike the ferromanganese crusts, the fish teeth also appear to preserve seawater Sr isotopes. There is not a perfect fit between the fish teeth data and the seawater curve, but some of the offset may represent errors in age estimates rather than alteration of the teeth. Relative to other potential proxies, fish teeth offer the added advantage that they can be found in deep sea sediment samples throughout the world's oceans throughout time. Therefore Sr and Nd isotopic paleoceanographic studies are not spatially or temporally limited.

Concentrations of Sr in the teeth appear to vary widely with the species of fish, although diagenetic incorporation of Sr can not be ruled out. In contrast, the large difference in Nd concentrations between the two sites is difficult to understand, but it clearly does not record progressive incorporation of Nd during burial. Instead sedimentation rate, the amount of time the teeth remain in contact with seawater, and possibly pore water concentrations may influence the amount of Nd incorporated into the teeth post-mortem.

Acknowledgments—We would like to thank Doug Macdougall, Chris MacIssac, and Pat Castillo of Scripps Institution of Oceanography for all their help with isotopic analyses. Vincent Salters at Florida State University also provided substantial assistance with analyses, as did Ann Heatherington at the University of Florida. Daniel Kuncicky picked many of the fish teeth. Peggy Delaney kindly taught E.E.M. the cleaning protocol employed in the study. Comments by Paul Mueller and thoughtful reviews by Charlie Jones and an anonymous reviewer substantially improved the manuscript. This research was funded by an NSF Career Award to E.E.M., as well as ACS-PRF grant #305430G2. Samples were provided by the Ocean Drilling Program.

REFERENCES

Abouchami W., Goldstein S. L., Galer S. J. G., Eisenhauer A., and Mangini A. (1997) Secular changes of lead and neodymium in central Pacific seawater recorded by a Fe-Mn crust. *Geochim. Cosmochim. Acta* **61,** 3957–3974.

Albaréde F. and Goldstein S. L. (1992) A world map of Nd isotopes in seafloor ferromanganese deposits. *Geology* **20,** 761–763.

Albaréde F., Goldstein S. L., and Dautel D. (1997) $^{143}Nd/^{144}Nd$ of Mn nodules from the Southern and Indian oceans, the global oceanic Nd budget, and their bearing on the deep ocean circulation during the Quarternary. *Geochim. Cosmochim. Acta* **61,** 1277–1291.

Aplin A., Michard A., and Albaréde F. (1986/87) $^{143}Nd/^{144}Nd$ in Pacific ferromanganese encrustations and nodules. *Earth Planet. Sci. Lett.* **81,** 7–14.

Berger W. H., Leckie R. M., Janecek T. R., Stax R., and Takayama T. (1993) Neogene carbonate sedimentation on Ontong Java Plateau: Highlights and open questions. In *Proc. ODP, Sci. Results* (ed. W. H. Berger, L. W. Kroenke, L. A. Mayer, et al.), **130,** 711–744.

Bernat M. (1975) Les isotopes de l'uranium et du thorium et les terres rares dans l'environment marine. *Cah. ORSTROM Ser. Geol.* **7,** 65–83.

Bertram C. J. and Elderfield H. (1993) The geochemical balance of the rare earth elements and neodymium isotopes in the oceans. *Geochim. Cosmochim Acta* **57,** 1957–1986.

Bertram C. J., Elderfield H., Aldridge R. J., and Morris S. C. (1992) $^{87}Sr/^{86}Sr$, $^{143}Nd/^{144}Nd$ and REEs in Silurian phosphatic fossils. *Earth Planet. Sci. Lett.* **113,** 239–249.

Birck J. L. (1986) Precision K-Rb-Sr isotopic analysis: Application to Rb-Sr chronology. *Chem. Geol.* **56,** 73–83.

Bloomer S. H., Taylor B., MacLeod C. J., Stern R. J., Fryer P., Hawkins J. W., and Johnson L. (1995) Early arc volcanism and the ophiolite problem: A perspective from drilling in the Western Pacific. *Geophys. Monograph* **88,** 1–30.

Boyle E. A. (1981) Cadmium, Zinc, Copper and Barium in foraminifera tests. *Earth Planet. Sci. Lett.* **53,** 11–35.

Boyle E. A. (1988) Cadmium: Chemical tracer of deepwater paleoceanography. *Paleoceanog.* **3,** 471–489.

Boyle E. A. and Keigwin L. D. (1985) Comparison of Atlantic and Pacific paleochemical records for the past 215,000 y: Changes in deep ocean circulation and chemical inventories. *Earth Planet. Sci. Lett.* **76,** 135–150.

Boyle E. A. and Keigwin L. D. (1987) North Atlantic thermohaline circulation during the last 20,000 years linked to high-latitude surface temperature. *Nature* **330,** 35–40.

Broecker W. S. and Peng T.-H. (1982) *Tracers in the Sea*. Eldigio Press.

Burnett W. C. (1990) Phosphorite growth and sediment dynamics in the Modern Peru shelf upwelling system. In *Neogene to Modern Phosphorites* (eds. W.C. Burnett and S.R. Riggs), pp.62–72, Cambridge Univ. Press.

Burton K. W., Ling H.-F., and O'Nions R. K. (1997) Closure of the Central American Isthmus and its effect on deep-water formation in the north Atlantic. *Nature* **386,** 382–385.

Cande S. C. and Kent D. V. (1995) Revised calibration of the geomagnetic polarity timescale for the Late Cretaceous and Cenozoic. *J. Geophys. Res.* **100(B4),** 6093–6095.

Curry W. B., Duplessy J. C., Labeyrie L. D., and Shackleton N. J. (1988) Changes in the distribution of $\delta^{13}C$ of deepwater ΣCO_2 between the last glaciation and the Holocene. *Paleoceanog.* **3,** 317–342.

Delaney M. L. (1990) Miocene benthic foraminiferal Cd/Ca Records. *Paleoceanog.* **5(5),** 743–760.

Elderfield, H. and Giekies, J. M. (1982) Sr isotopes in interstitial waters of marine sediments from Deep Sea Drilling Project cores. *Science* **300,** 493–497.

Elderfield H. and Greaves M. J. (1982) The rare earth elements in seawater. *Nature* **296,** 214–219.

Elderfield H. and Pagett R. (1986) Rare earth elements in ichthyoliths: Variations with redox conditions and depositional environments. *Sci. Tot. Env.* **49,** 175–197.

Elderfield H., Upstill-Goddard R., and Sholkovitz E. R. (1990) The rare earth elements in rivers, estuaries, and coastal seas and their significance to the composition of ocean waters. *Geochim. Cosmochim. Acta* **54,** 971–991.

Elderfield H., Hawkesworth C. J., Greaves M. J., and Calvert S. E. (1981) Rare earth element geochemistry of oceanic ferromanganese nodules and associated sediments. *Geochim. Cosmochim. Acta* **45,** 513–528.

Farrell J. W., Clemens, S. C., and Gromet, L. P. (1995) Improved chronostratigraphic reference curve of late Neogene seawater $^{87}Sr/^{86}Sr$. *Geology* **23,** 403–406.

Felitsyn S., Sturesson U., Popov L., and Holmer L. (1998) Nd isotope composition and rare earth element distribution in early Paleozoic biogenic apatite from Baltoscandia: A signature of Iapetus ocean water. *Geology* **26,** 1083–1086.

Fryer P., Pearce J. A., Stokking L. B., et al. (1990) Site 786. In *Proc. ODP Init. Repts.*, **125,** 819–363.

Gieskes J. M. (1981) Deep-sea drilling interstitial water studies: Implications for chemical alteration of the oceanic crust, Layers I and II. In *The Deep Sea Drilling Project: A Decade of Progress* (eds. J. E. Warme, R. G. Douglas, E. L. Winterer) *Spec. Pub., Soc. Econ. Paleontol. Mineral.* **32,** 149–167.

Goldstein S. J. and Jacobsen S. B. (1988) Nd and Sr isotope systematics of river water suspended material: Implications for crustal evolution. *Earth Planet. Sci. Lett.* **87,** 249–265.

Goldstein S. L., O'Nions R. K., and Hamilton P. J. (1984) A Sm-Nd isotopic study of atmospheric dusts and particulates from major river systems. *Earth Planet. Sci. Lett.* **70,** 221–236.

Grandjean P., Cappetta H., Michard A., and Albaréde F. (1987) The assessment of REE patterns and $^{143}Nd/^{144}Nd$ ratios in fish remains. *Earth Planet. Sci. Lett.* **84,** 181–196.

Halliday A. N., Davidson J. P., Holden P., Owen R. M., and Olivarez A. M. (1992) Metalliferous sediments and the scavenging residence time of Nd near hydrothermal vents. *Geophys. Res. Lett.* **19,** 761–764.

Haug, G. H. and Tiedemann, R. (1998) Effect of the formation of the Isthmus of Panama on Atlantic Ocean thermohaline circulation. *Nature* **393,** 673–676.

Hay, W. W. (1996) Tectonics and climate. *Geol. Rundsch.* **85,** 409–437.

Hein J. R., Halbach P., Manheim F. T., Bau M., Kang J.-K., and Lubick N. (1997) Iron and Manganese oxide mineralization in the Pacific. In *Manganese mineralization: Geochemistry and Mineralogy of Terrestrial and Marine Deposits* (eds. K. Nicholson, J. R. Hein, B. Buhn, and S. Dasgupta), *Geol. Soc. Spec. Pub.* **119,** 123–138.

Hemming S. R., Goldstein S. L., and Rutberg R. (1998) Survey of the Nd isotope composition of ferromanganese precipitates from marine sediment core-tops. *6th International Conf. on Paleoceanography*, **122** (abstr.).

Hodell D. A. and Woodruff F. (1994) Variations in the strontium isotopic ratio of seawater during the Miocene: Stratigraphic and geochemical implications. *Paleoceanog.* **9,** 405–426.

Ingram B. L., Hein J. R., and Farmer G. L. (1990) Age determinations and growth rates of Pacific ferromanganese deposits using strontium isotopes. *Geochim. Cosmochim. Acta* **54,** 1709–1721.

Jacobsen S. B. and Wasserburg G. J. (1980) Sm-Nd isotopic evolution of chondrites. *Earth Planet. Sci. Lett.* **50,** 139–155.

Jeandel C. (1993) Concentration and isotopic compositions of Nd in the South Atlantic Ocean. *Earth and Planet. Sci. Lett.* **117,** 581–591.

Jeandel C., Bishop J. K., and Zindler A. (1995) Exchange of neodymium and its isotopes between seawater and small and large particles in the Sargasso Sea. *Geochim. Cosmochim. Acta* **59,** 535–547.

Jeandel C., Thouron D., and Fieux M. (1998) Concentrations and isotopic compositions of neodymium in the eastern Indian Ocean and Indonesian straits. *Geochim. Cosmochim. Acta* **62,** 2597–2607.

Jones C. E., Halliday A. N., Rea D. K., and Owen R. M. (1994) Neodymium isotopic variations in North Pacific modern silicate sediment and the insignificance of detrital REE contributions to seawater. *Earth Planet. Sci. Lett.* **127,** 55–66.

Keigwin L. D. (1982) Isotopic Paleoceanography of the Caribbean and East Pacific: Role of Panama Uplift in Late Neogene Time. *Science* **217,** 350–353.

Kennett J. P. (1977) Cenozoic evolution of Antarctic Glaciation, the Circum-Antarctic Ocean and their impact on global paleoceanography. *J. Geophys. Res* **82,** 3843–3860.

Kennett J. P. (1982) *Marine Geology*. Prentice-Hall.

Keto L. S. and Jacobsen S. B. (1987) Nd and Sr isotopic variations of Early Paleozoic oceans. *Earth Planet. Sci. Lett.* **84,** 27–41.

Krissek L. A. and Janecek T. R. (1993) Eolian deposition on the Ontong Java Plateau since the Oligocene: Unmixing a record of multiple dust sources. In *Proc. ODP, Sci. Results* (eds. W. H. Berger, L. W. Kroenke, and L. A. Mayer), **130,** 471–490.

Kroenke L. W., Berger W. H., and Janecek T. R. (1991) Site 807. In *Proc. ODP, Init. Repts.*, **130,** 369–496.

Ku T. L. and Broecker W. S. (1967) Uranium, thorium and protactinium in a manganese nodule. *Earth Planet. Sci. Lett.* **2,** 317–321.

Ling H. F., Burton K. W., O'Nions R. K., Kamber B. S., von Blankenburg F., Gibb A. J., and Hein J. R. (1997) Evolution of Nd and Pb isotopes in Central Pacific seawater from ferromanganese crusts. *Earth Planet. Sci. Lett.* **146,** 1–12.

Maier-Reimer E., Mikolajewicz U., and Crowley T. (1990) Ocean general circulation model sensitivity experiment with an open Central American Isthmus. *Paleoceanog.* **5,** 349–366.

Martin E. E. and Macdougall J. D. (1995) Sr isotopes at the Permian/Triassic boundary: A record of climate change. *Chem. Geol.* **125,** 73–99.

Martin E. E., Macdougall J. D., Herbert T. D., Paytan A., and Kastner M. (1995) Sr and Nd isotopic analyses of marine barite separates. *Geochim Cosmochim Acta* **59,** 1353–1361.

Martin E. E., Shackleton N. J., Zachos J. C., and Flower B. P. (1999) Orbitally-tuned Sr isotope chemostratigraphy for the late middle to late Miocene. *Paleoceang.* **14,** 74–83.

McDuff R. and Gieskes J. M. (1976) Calcium and Magnesium profiles in DSDP interstitial waters: Diffusion or reaction? *Earth Planet. Sci. Lett.* **33,** 1–10.

Mead, G. A. (1996) Correlations of Cenozoic-Late Cretaceous geomagnetic polarity time scales: And internet archive. *J. Geophys. Res.***101(B4),** 8107–8109.

Mead G. A. and Hodell D. A. (1995) Controls on the $^{87}Sr/^{86}Sr$ composition of seawater from the Middle Eocene to Oligocene: Hole 689B, Maud Rise, Antarctica. *Paleoceanog.* **10,** 327–346.

Michard A., Albaréde F., Michard G., Minster J. F., and Charlou J. L. (1983) Rare-earth elements and uranium in high-temperature solutions from East Pacific Rise hydrothermal vent field (13°N). *Nature* **303,** 795–797.

Mikolajewicz U. and Crowley T. J. (1997) Response of a coupled ocean/energy balance model to restricted flow through the Central American isthmus. *Paleoceanog.* **12,** 429–441.

Mikolajewicz U., Maier-Reimer E., Crowley T. J., and Kim K.-Y.

(1993) Effect of Drake and Panamanian Gateways on the circulation of an ocean model. *Paleoceanog.* **8,** 409–426.

Mottl M. J. and Alt J. C. (1992) Data Report: Minor and trace element and sulfur isotopic composition of pore waters from Sites 778 through 786. In *Proc. ODP Sci. Results* (eds. P. Fryer, J. A. Pearce, L. B. Stokking, et al.), **125,** 683–688.

O'Nions R. K., Frank M., von Blanckenburg F., and Ling H.-F. (1998) Secular variation of Nd and Pb isotopes in ferrmanganese crusts from the Atlantic, Indian and Pacific Oceans. *Earth Planet. Sci. Lett.* **155,** 15–28.

Palmer M. R. (1985) Rare earth elements in foraminifera tests. *Earth Planet. Sci. Lett.* **73,** 285–298.

Palmer M. R. and Elderfield H. (1985) Variations in the Nd isotopic composition of foraminifera from Atlantic Ocean sediments. *Earth Planet. Sci. Lett.* **73,** 299–305.

Palmer M. R. and Elderfield H. (1986) Rare earth elements and neodymium isotopes in ferromanganese oxide coatings of Cenozoic foraminifera from the Atlantic Ocean. *Geochim. Cosmochim. Acta* **50,** 409–417.

Pearce J. A., Thirwall M. F., Ingram G., Murton B. J., Arculus R. J., and van der Laan S. (1992) Isotopic evidence for the origin of boninites and related rocks drilled in the Izu-Bonin (Osagawara) forearc, Leg 125. In *Proc. ODP, Sci. Results* (eds. P. Fryer, J. A. Pearce, L. B. Stokking, et al.), **125,** 237–262.

Pickard G. L. and Emery W. J. (1990) *Descriptive Physical Oceanography*. Pergamon Press.

Piepgras D. J. and Jacobsen S. B. (1988) The isotopic composition of neodymium in the North Pacific. *Geochim. Cosmochim. Acta* **52,** 1373–1381.

Piepgras D. J. and Wasserburg G. J. (1982) Isotopic composition of neodymium in waters from the Drake Passage. *Science* **217,** 207–214.

Piepgras D. J. and Wasserburg G. J. (1985) Strontium and neodymium isotopes in hot springs on the East Pacific Rise and Guaymas Basin. *Earth Planet. Sci. Lett.* **72,** 341–356.

Piepgras D. J. and Wasserburg G. J. (1987) Rare earth element transport in the western North Atlantic inferred from Nd isotopic observations. *Geochim. Cosmochim. Acta* **51,** 1257–1271.

Raymo M. E., Ruddiman W. F., Shackleton N. J., and Oppo D. W. (1990) The evolution of Atlantic-Pacific $\delta^{13}C$ gradients over the last 2.5 Myrs: Evidence of decoupling of deep water circulation and global ice volume changes *Earth Planet. Sci. Lett.* **97,** 353–368.

Resig J. M., Buyannononth V., and Roy K. J. (1976) Foraminiferal stratigraphy and depositional history in the area of Ontong Java Plateau. *Deep Sea Res.* **23,** 441–456.

Richter, F. M. and DePaolo, D. J. (1988) Diagenesis and Sr isotopic evolution of seawater using data from DSDP 590B and 575. *Earth Planet. Sci. Lett.* **90,** 382–394.

Richter, F. M. and Liang, Y. (1993) The rate and consequences of Sr diagenesis in deep-sea carbonates. *Earth Planet. Sci. Lett.* **117,** 553–565.

Rutberg R., Hemming S., and Goldstein S. L. (1997) Deconvolving the detrital and marine radiogenic isotope records from deep sea cores: Implications for paleocean circulation studies. *EOS* **78,** F376 (abstr.).

Schmitz B., Aberg G., Werdelin L., Forey P., and Bendix-Almgreen S. E. (1991) $^{87}Sr/^{86}Sr$, Na, F, Sr, and La in skeletal fish debris as a measure of the paleosalinity of fossil-fish habitats. *Geol. Soc. Amer. Bull.* **103,** 786–794.

Shackleton N. J., Imbrie J., and Hall M. A. (1983) Oxygen and carbon isotope record of East Pacific core V19–30: Implications for the formation of deep water in the late Pleistocene North Atlantic. *Earth Planet Sci. Lett* **65,** 233–244.

Shaw H. F. and Wasserburg G. J. (1985) Sm-Nd in marine carbonates and phosphates: Implications for Nd in seawater and crustal ages. *Geochim. Cosmochim. Acta* **54,** 2433–2438.

Shemesh A. (1990) Crystallinity and diagenesis of sedimentary apatites. *Geochim. Cosmochim. Acta* **54,** 2433–2438.

Shimizu H., Tachikawa K., Masuda A., and Nozaki Y. (1994) Cerium and neodymium isotope ratios and REE patterns in seawater from the North Pacific Ocean. *Geochim. Cosmochim. Acta* **58,** 323–333.

Sholkovitz E. R. (1993) The geochemistry of rare earth elements in the Amazon River estuary. *Geochim. Cosmochim. Acta* **58,** 2181–2190.

Snoeckx, H., Rea, D. K., Jones, C. E. and Ingram, B. L. (1995) Eolian and silica deposition in the central north Pacific: Results from Leg 145 Sites 885/886. In *Proc. ODP, Sci. Results* (eds. D. K. Rea, I. A. Basov, D. W. Scholl, and J. F. Allan), **145,** 219–230.

Stabell B., Ali J., Ciampo G., Milner G., Wang Y.-J., and Xu Y. (1992) Biostratigraphic Summary, Leg 125. (eds. P. Fryer, J. A. Pearce and L. B. Stokking), **125,** 615–621.

Staudigel H., Doyle P., and Zindler A. (1985) Sr and Nd isotope systematics in fish teeth. *Earth Planet. Sci. Lett.* **76,** 45–56.

Stille P. (1992) Nd-Sr isotope evidence for dramatic changes of paleocurrents in the Atlantic Ocean during the past 80 m.y. *Geolog.* **20,** 387–390.

Stille P. and Fischer H. (1990) Secular variation in the isotopic composition of Nd in Tethys seawater. *Geochim. Cosmochim. Acta* **54,** 3139–3145.

Stille P., Steinmann M., and Riggs S., R. (1996) Nd isotope evidence for the evolution of the paleocurrents in the Atlantic and Tethys Oceans during the past 180 Ma. *Earth Planet. Sci. Lett.* **144,** 9–19.

VonderHarr D. L., Mahoney J. J., and McMurtry G. M. (1995) An evaluation of strontium isotopic dating of ferromanganese oxides in a marine hydrogenous ferromanganese crust. *Geochim. Cosmochim. Acta* **59,** 4267–4277.

Woodruff F. and Savin S. M. (1989) Miocene deepwater oceanography. *Paleoceanog.* **4,** 87–140.

Wright J., Schrader H., and Holser W. T. (1987) Paleoredox variations in ancient oceans recorded by rare earth elements in fossil apatite. *Geochim. Cosmochim. Acta* **51,** 631–644.

Wright J., Seymour R. S., and Shaw H. F. (1984) REE and Nd isotopes in conodont apatite: Variations with geological age and depositional environment. In *Conodont Biofacies and Provincialism* (ed. D. L. Clark), *Geol. Soc. Amer. Spec. Pap.*, **196,** 325–340.

Xu, Y. and Wise, S. W., Jr. (1992) Middle Eocene to Miocene calcareous nannofossils of Leg 125 from the western Pacific Ocean. In *Proc. ODP, Sci. Results* (eds. P. Fryer, J. A. Pearce, L. B. Stokking, et al.), **125,** 43–70.